CONCRETE LIBRARY OF JSCE NO. 36, DECEMBER 2000

ANALYSIS OF BONDING AND DELAMINATING BEHAVIOR OF CONTINUOUS FIBER SHEET BONDED ON CONCRETE

(Translation from Proceedings of JSCE, No. 634/V-45, November 1999)

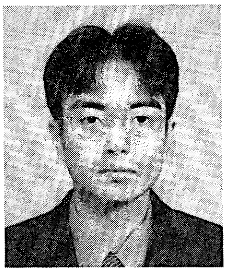
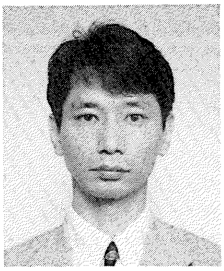
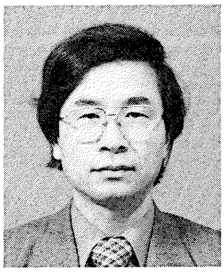
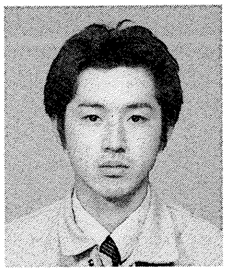

Akihisa KAMIHARAKO　Takumi SHIMOMURA　Kyuichi MARUYAMA　Hiroyuki NISHIDA

Test of bond between continuous fiber (CF) sheet and concrete are used to develop constitutive model that simulate the bonding behavior of CF sheet. The resulting bilinear and cut-off models take into account the relationship between shear stress and shear displacement. A numerical simulation of the bond tests was implemented so as to carried out verification and sensitively analysis of the models. The models are shown to be capable of predicting the actual bonding and delaminating behavior of CF sheet bonded to concrete.

***Keywords:** CF sheet, Bonding, Constitutive model of bond characteristics, Bilinear model, Cut-off model, Numerical simulation*

Akihisa Kamiharako is a graduate student at Nagaoka University of Technology, Japan. His research interests include the structural behavior and repair or strengthening of reinforced concrete and the seismic design of concrete structures. He is a member of the JSCE and JCI.

Takumi Shimomura is an associate professor at Nagaoka University of Technology. His research interests include concrete drying shrinkage, numerical simulation of deterioration process of concrete structures, and retrofit design for concrete structures. He is a member of the JSCE, JCI, ACI, RILEM, and fib.

Kyuichi Maruyama is a professor at Nagaoka University of Technology. His current research interests are the retrofitting of RC members with continuous fiber sheet, seismic design, self-compacting concrete, and the recycling of waste materials. He is a member of the JSCE, JCI, AIJ, ACI, and IABSE.

Hiroyuki Nishida is a former graduate student at Nagaoka University of Technology. He is currently working for Oriental Corporation Ltd. of Japan as a design engineer. His current research interests relate to composite materials and structures.

---

1. INTRODUCTION

One method of repair or strengthening of existing reinforced concrete structures is retrofitting with continuous fiber (CF) sheeting. A great deal of research has been carried out in this field, and design recommendations based on state-of-the-art literature have been established in Japan[1][2][3]. To evaluate the deformation and failure behavior of retrofitted structural members, it is necessary to develop an understanding of the bonding and delaminating behavior of the CF sheet and concrete as pointed out by both Sato et al.[4] and Wu et al.[5]. Based on computational model for estimating the bonding and delaminating state of the CF sheet, the authors have attempted to evaluate the shear capacity of retrofitted reinforced concrete members[6]. This method provides sufficiently accurate predictions of ultimate shear capacity.

To predict the bonding and delaminating behavior of the CF sheet-concrete system, a constitutive model that takes into account the bonding characteristics at the boundary between CF sheet and concrete is needed in the computational analyses. The best-known model is the relationship between shear stress and shear displacement with bilinear and cut-off implementations both being used. Most researchers, including the authors, adopt both variations of the model in conducting computational analysis[4][6][7]. Neither model, however, would accurately represent actual behavior.

This study will focus on explaining the actual bonding and delaminating behavior of the bond between CF sheet and concrete, and a derivation of constitutive model is proposed. The models are derived from a strain distribution obtained as a result of bond tests on the CF sheet-concrete system. The bond tests are also simulated by computational methods based on the models, thus enabling. There are conducted as sensitively analysis of the models. This study method is summarized in Fig. 1.

2. BONDING TESTS ON CONTINUOUS FIBER SHEET AFFIXED TO CONCRETE

2.1 Test method

The bond tests carried out by the authors were based on the method proposed by the Japan Concrete Institute's Technical Committee on Continuous Fiber Reinforced Concrete (JCI-TC952)[2]. Details of 18 specimens and the results of the tests are summarized in Table 1. The experimental parameters included type of CF sheet (carbon or aramid fiber), bonded length and width of CF sheet, and the elastic modulus of the epoxy resin. The material properties are summarized in Table 2.

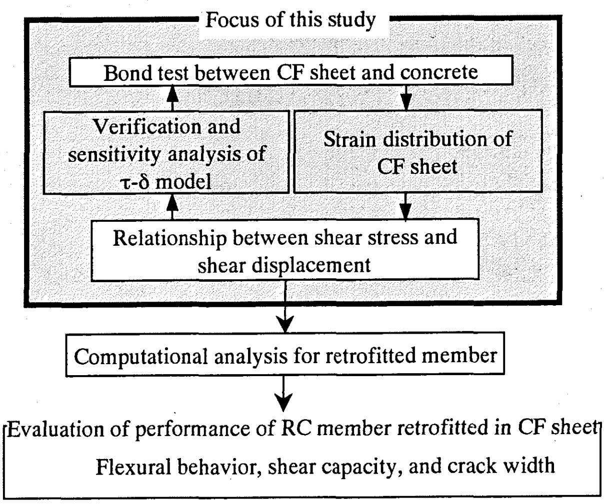

Fig. 1 Current and future works

Table 1 Summary of experimental program

Specimen	CF sheet	Epoxy resin	Bonded width of CF sheet (mm)	Bonded length of CF sheet (mm)	Number of layer	Compressive strength of concrete (N/mm^2)	Surface treatment	Ultimate load (kN)	Failure mode
S1-1	C	EA	10	145	1	34.9	Sanding	6.25	Rupture*
S1-2	C	EA	10	250	1	36.3	Sanding	5.78	Rupture
S1-3	C	EA	20	145	1	36.3	Sanding	9.84	Rupture
S1-4	C	EA	20	175	1	36.3	Sanding	8.78	Delaminating**
S1-5	C	EA	30	100	1	34.9	Sanding	12.89	Delaminating
S1-6	C	EA	30	175	1	34.9	Sanding	14.71	Rupture
S1-7	C	EA	30	250	1	38.8	Sanding	12.83	Delaminating
S1-8	C	EA	50	250	1	36.3	Sanding	22.52	Rupture
S1-9	C	EA	70	175	1	41.5	Sanding	29.84	Delaminating
S1-10	C	EA	90	175	1	41.5	Sanding	29.38	Delaminating
S2-1	A	EA	30	175	1	38.8	Sanding	9.93	Delaminating
S2-2	A	EA	30	200	1	36.5	Sanding	10.01	Delaminating
S3-1	C	EB	30	175	1	42.4	Sanding	14.25	Rupture
S3-2	A	EB	30	200	1	36.5	Sanding	14.7	Delaminating
S4-1	C	EA	30	175	2	35.1	Sanding	28.91	Delaminating
S5-1	C	EA	30	175	1	53.4	Sanding	17.45	Rupture
S5-2	C	EA	30	175	1	75.5	Sanding	9.68	Delaminating
S6-1	C	EA	30	175	1	42.4	No sanding	12.16	Delaminating

*CF sheet ruptured in ultimate state, **CF sheet bonded testing length was delaminated over whole length

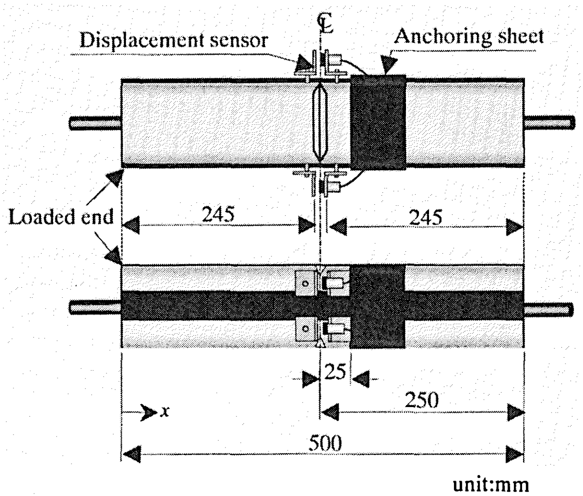

Fig. 2 Test specimen

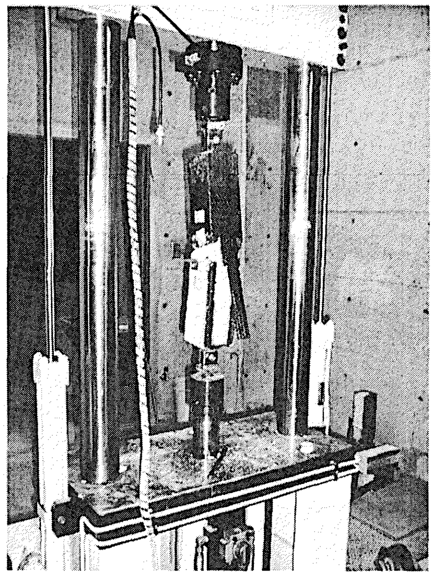

Fig. 3 Testing method

The method used for bonding the CF sheet to the concrete conformed to JCI-TC952. The surface of the prismatic concrete was treated with a grinder to remove laitance, and then the corners were rounded off. Further, both surfaces were primed with resin before bonding strips of CF sheet to the surfaces with epoxy resin.

The specimen dimensions are shown in Fig.2. All specimens were 100mm square in cross section and 500mm in length. The tested length was a half span from the center. The remaining length was anchored by bonding with CF sheet measuring 150mm in width so as to ensure no delaminating took place in this portion. An unbonded region measuring 50mm in width (i.e. 25mm from the center in each direction) was left at the center of the specimen to allow wrapping with aluminum tape. To direct the major crack, grooves measuring 15mm in width and 7.5mm in depth were formed along the center of the lateral surfaces.

Table 2 Material properties

Symbol	Material	Thickness (mm)	Tensile strength (N/mm^2)	Elastic modulus (kN/mm^2)
C	Carbon fiber sheet	0.111	3500	270
A	Aramid fiber sheet	0.169	2800	80
EA	Epoxy resin A	N/A	50.3	1.5
EB	Epoxy resin B	N/A	12.5	0.7

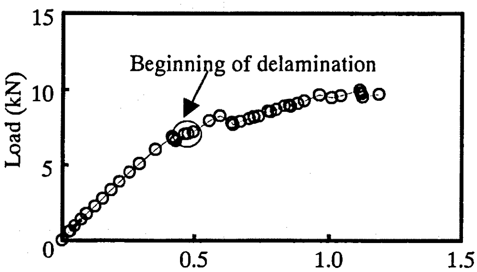

Fig. 4 Load - displacement curve (specimen S1-3)

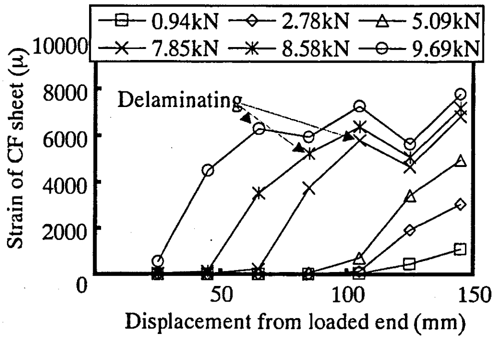

Fig. 5 Strain distribution of CF sheet at every loading step (specimen S1-3)

The testing machine was an actuator of 50kN capacity as shown in Fig.3. Loading was by stroke control at a rate of 0.05mm/min. The tensile force was applied to the specimen by pulling on embedded steel bars.

Measurements included loads, opening displacement at mid span (i.e. crack width at the center position), and CF sheet strain. The loads was measured with a load cell, which was integral to the actuator. The opening displacement was acquired using displacement sensors placed on faces opposite the bonded CF sheets (two sensors per face, for a total of four sensors per specimen). CF sheet strain was measured with strain gages affixed to the surface of the CF sheet at a spacing of 20mm.

2.2 Test results

Examples of test results are shown in Figs. 4 and 5, the former giving the load-opening displacement at mid span and the latter showing the strain distribution over the CF sheet at several loading steps. A full and comprehensive consideration of these results is reported in Reference [8], and only an outline is given here. The load did not increase very much after delamination began. However, the bonding stiffness decreased. This is possibly because the shear stress is distributed over a limited length. This observation has been reported by Satoh et al.[4].]

The strain distribution corresponding to delamination was not uniform. The reason for this is that the CF sheet delaminated at the bonded face along with a thin layer of concrete fragments, which remained attached to the sheet. As a result, the stiffness of the CF sheet was greater where fragments adhered to it.

3. DERIVATION OF SHEAR STRESS VERSUS SHEAR DISPLACEMENT RELATIONSHIP

3.1 Formulation

The relationships between shear stress and shear displacement was obtained the acquired CF sheet strain using the method given here. First, the loaded ends are defined as the two ends of the concrete block. the origin in the axial direction, x=0, is defined as the loaded end at the left side (see Fig. 2).

a) Shear displacement

The shear displacement between CF sheet and concrete at point can be calculated using the following formula:

$$\delta(x) = u_{cf}(x) - u_c(x) \tag{1}$$

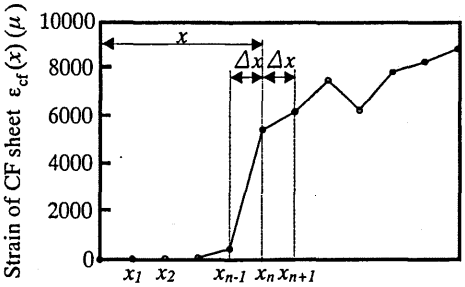

Fig.6 Strain distribution for calculating τ-δ relationships (From acquired data)

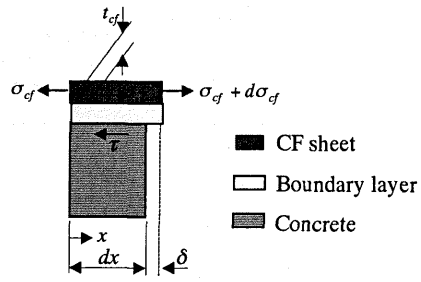

Fig. 7 Equilibrium of stress in specimen

where $u_{cf}(x)$ and $u_c(x)$ are the displacements of the CF sheet and the concrete, respectively.

Considering the difference in stiffness between CF sheet and concrete (see Chapter 4), it is assumed that concrete is a rigid body. The concrete strain and absolute displacement should therefore be equal to zero, so Eq. (1) can be rearranged as

$$\delta(x) = u_{cf}(x) \tag{2}$$

An example of a measured strain distribution is shown in Fig. 6. The displacement of the CF sheet, i.e. the shear displacement, is calculated by integrating the measured strain distribution:

$$\begin{aligned} u_{cf}(x) &= \int_0^x \varepsilon_{cf}(x)dx \\ &= \frac{\Delta x}{2}\left(\varepsilon_{cf}(x_0) + 2\sum_{i=1}^{n-1}\varepsilon_{cf}(x_i) + \varepsilon_{cf}(x_n)\right) \end{aligned} \tag{3}$$

where Δx is the spacing of strain gages, and $\varepsilon_{cf}(x_0)$, $\varepsilon_{cf}(x_i)$, and $\varepsilon_{cf}(x_n)$ are the measured CF sheet strains at the measuring points.

b) Shear stress

The stress equilibrium is shown in Fig. 7. The equilibrium condition can be derived as

$$t_{cf} \cdot \frac{d\sigma_{cf}(x)}{dx} - \tau(x) = 0 \tag{4}$$

where t_{cf} is the CF sheet thickness and $\sigma_{cf}(x)$ is the tensile stress of a unit width of CF sheet.

On the assumption that the CF sheet is an elastic body, its constitutive relationship is

$$\sigma_{cf}(x) = E_{cf} \cdot \varepsilon_{cf}(x) \tag{5}$$

where $\sigma_{cf}(x)$ and $\varepsilon_{cf}(x)$ are the CF sheet stress and strain, respectively, and E_{cf} is the elastic modulus of the CF sheet.

By means of Eq. (5) and the acquired data, Eq. (4) can be rearranged as

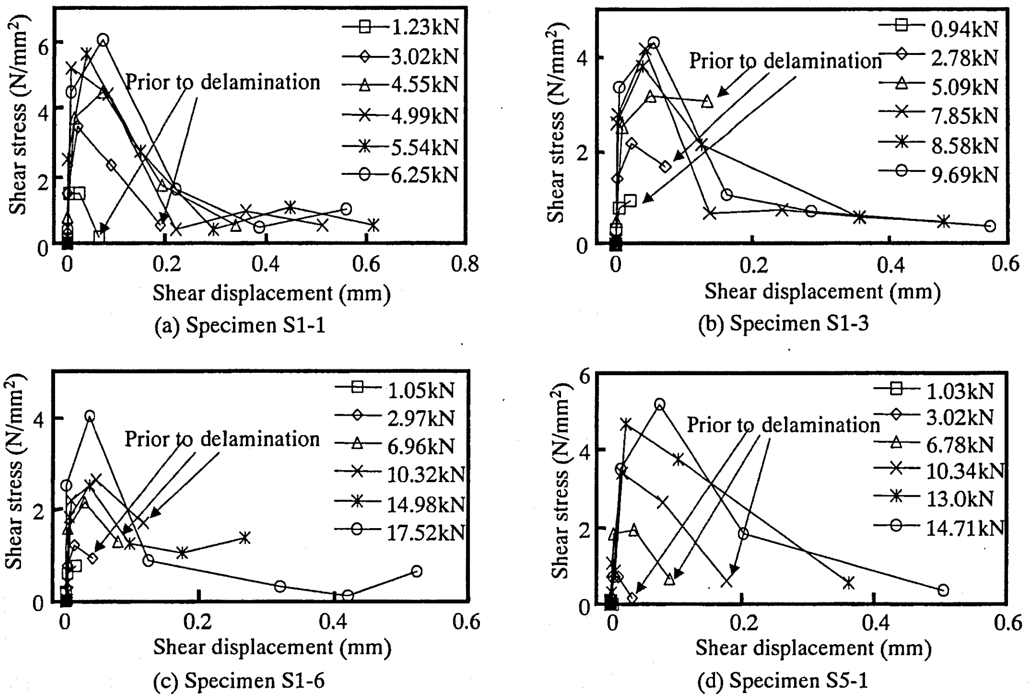

(a) Specimen S1-1
(b) Specimen S1-3
(c) Specimen S1-6
(d) Specimen S5-1

Fig. 8 Examples of shear displacement and shear stress relationships

$$\begin{aligned}\tau(x) &= E_{cf} \cdot t_{cf} \cdot \frac{d\varepsilon_{cf}(x)}{dx} \\ &\cong E_{cf} \cdot t_{cf} \cdot \left(\frac{\varepsilon_{cf}(x_{n+1}) - \varepsilon_{cf}(x_{n-1})}{\Delta x} \right)\end{aligned} \tag{6}$$

The shear stress obtained by Eq. (6) might be affected by the strain gage spacing. According to Reference 2, the distributed length of shear stress, as well-known effective bond length, would be distributed around 20 to 100mm. If the gage spacing ware less than 20mm, the obtained stress would not be affected.

The shear stress and shear displacement at each loading step and measuring point can be obtained using Eq. (3) and Eq. (6), respectively. The following are two alternatives for developing the relationship:
Alternative 1: Calculating the relationship at each strain gage location
Alternative 2: Calculating the relationship at each loading step
A derivation using only Alternative 2 will be given in this study (see section 3.3), since the authors have previously reported that Alternative 1 is not suitable.

3.2 Calculation results

Examples of calculation results are shown in Fig. 8. After delamination is initiated, the curves considered of softening and elastic zones, and those converged on the same points. The softening zone appears in some curves prior to delamination. This is because a strain gradient is formed as a result of the unbonded length at the center of the specimen. It does not affect the delamination behavior of the CF sheet.

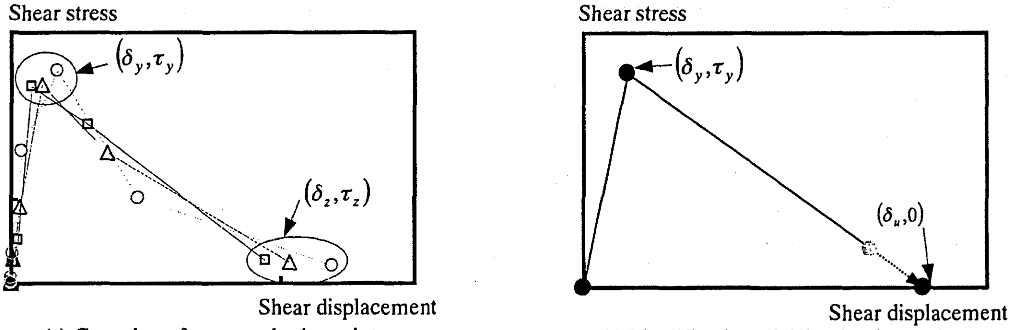

(a) Grouping of max. and min. point

(b) Identification of delamination point

Fig. 9 Modeling of shear stress and shear displacement relationships

Fig. 3 Material parameters of whole specimen

Specimen	CF sheet	Epoxy resin	Bonded width of CF sheet (mm)	Bonded length of CF sheet (mm)	Number of layers	Surface treatment	Compressive strength of concrete (N/mm^2)	Material parameter of model		
								δ_y (mm)	τ_y (N/mm^2)	δ_u (mm)
S1-1	CF	EA	10	145	1	Sanding	34.9	0.043	4.76	0.40
S1-2	CF	EA	10	250	1	Sanding	36.3	0.053	5.56	0.49
S1-3	CF	EA	20	145	1	Sanding	36.3	0.035	4.17	0.43
S1-4	CF	EA	20	175	1	Sanding	36.3	0.040	3.17	0.54
S1-5	CF	EA	30	100	1	Sanding	34.9	0.030	4.19	0.32
S1-6	CF	EA	30	175	1	Sanding	34.9	0.044	4.69	0.40
S1-7	CF	EA	30	250	1	Sanding	38.8	0.039	3.19	0.40
S1-8	CF	EA	50	250	1	Sanding	36.3	0.053	4.30	0.34
S1-9	CF	EA	70	175	1	Sanding	41.5	0.052	3.11	0.37
S1-10	CF	EA	90	175	1	Sanding	41.5	0.028	2.93	0.28
S2-1	AF	EA	30	175	1	Sanding	38.8	0.052	4.56	0.58
S2-2	AF	EA	30	200	1	Sanding	36.5	0.057	3.21	0.55
S3-1	CF	EB	30	175	1	Sanding	42.4	0.310	4.47	-*
S3-2	AF	EB	30	200	1	Sanding	36.5	0.061	2.96	0.56
S4-1	CF	EA	30	175	2	Sanding	35.1	0.042	3.74	0.40
S5-1	CF	EA	30	175	1	Sanding	53.4	0.031	3.27	0.31
S5-2	CF	EA	30	175	1	Sanding	75.5	0.043	4.20	0.36
S6-1	CF	EA	30	175	1	No sanding	42.4	0.032	3.50	0.27

*Softening part did not appear because CF sheet ruptured prior to delamination.

3.3 Elastic-softening-delamination model (bilinear model)

The curves obtained from the above procedure are modeled using a bilinear function. This function consists of elastic and softening parts. The derivation is as follows.
1st step: The delamination initiation point is identified from the load-opening displacement curve (see Fig. 4).
2nd step: The points corresponding to maximum and minimum shear stress are grouped on the curve (see Fig. 9).
3rd step: The averaged points, (δ_y, τ_y), and (δ_z, τ_z) are calculated from the acquired data as grouped in the second step. The shear displacement corresponding to the start of delamination is then identified by extrapolation (see Fig. 9(b)).
4th step: A series of calculations is carried out for the data on both sides. The averages of, δ_y, τ_y, and δ_u, are calculated from the results for both sides.

The identified parameters, τ_y, δ_y and δ_u, for all specimen are summarized in Table 3. The factors influencing the bilinear model are discussed below[8].

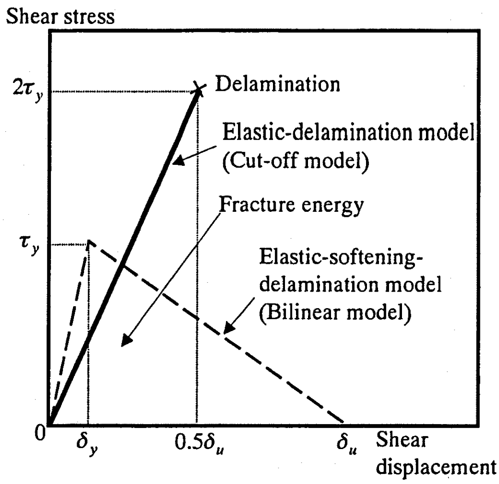

Fig. 10 Identification for elastic-delamination model

a) Compressive strength of concrete
Even with increasing concrete strength, the identified parameters did not change excessively. The bonding characteristics of CF sheet are related closely to its resistance todelamination (see Section 2.2).
b) Surface treatment
The stress, τ_y, and displacement, δ_u, were lower in cases where no surface sanding was carried out. Where no such treatment was carried out, the aggregate was not fully exposed completely at the surface, and as a result bonding between CF sheet and concrete was inadequate.
c) Bond width of CF sheet
As long as the bonding width was greater than 10mm, all identified parameters remained almost constant. However, the stress, τ_y, increased when the width was less than 10mm. From the experimental investigation, it was determined that the failure zone of the mortar layer was greater than the bonding width. The stress might be affected by this phenomenon.
d) Bond length of CF sheet
The identified parameters do not change significantly when the bond length is 100mm to 250mm, because the effective bond length is less than 100mm (see Section 3.1).
e) Number of bond layers of CF sheet
Comparing the identified parameter for two bonded layers of CF sheet with the parameter for a single layer, no significant change is noted. There is adequate bonding between the first layer and second layers, so laminated CF sheets is showed similar delamination behavior to the single layer.
f)Elastic modulus of epoxy resin
When CF sheet was bonded with the epoxy resin of lower elastic modulus, the sheet ruptured at mid span prior to delamination, and ultimately it was impossible to obtain the identified parameter. This observation implies that displacement, δ_u, which is the delaminating criterion, is higher in the case of this resin. The identified parameter, however, does not depend on the epoxy resin's elastic modulus in the case of specimens, S2-1, S2-2, and S2-3 with bonded aramid fiber sheet. These results cannot yet be explained rationally because more investigations of the epoxy resins are required.

3.4 Elastic-delamination model (Cut-off model)

The bilinear model is a rigorous procedure that is capable of predicting delamination behavior. However this rigorous approach requires a complicated analysis. To compare the accuracy of a simplified method of analysis against this rigorous method, a cut-off model is also discussed. The cut-off model is derived very simply: the fracture energy, which is the area of the triangular section in the case of the bilinear model, should be made the same as in the bilinear model. A schematic of this is shown in Fig. 10. In the cut-off model will provide almost the same results as the rigorous procedure.

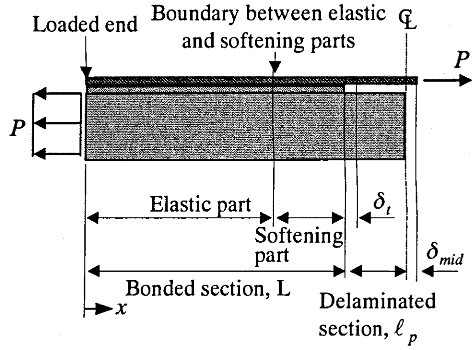

Fig. 11 One-dimensional CF sheet-concrete system

Table 4 Boundary conditions

	State	Boundary conditions
Bilinear model	I	$x = 0 : \sigma_{cf} = 0, x = L : \delta = \delta_t$ for Eq. (11)
	II, III	$x = 0 : \sigma_{cf} = 0, x = \ell_e : \delta = \delta_y$ for Eq.(11) $x = \ell_e : \delta = \delta_y, x = L : \delta = \delta_t$ for Eq. (12)
Cut-off model	N/A	$x = 0 : \sigma_{cf} = 0, x = L : \delta = \delta_t$ for Eq. (13)

4. COMPUTATIONAL SIMULATION OF BOND TEST

4.1 Formulation

The stress-strain relationship for the CF sheet is

$$\varepsilon_{cf}(x) \equiv \frac{du_{cf}(x)}{dx} \tag{7}$$

Constitutive relationships are required to determine the shear stress from the shear displacement. For the bilinear model, these relationships are

$$\tau = \begin{cases} \dfrac{\tau_y}{\delta_y} \cdot \delta & (0 \le \delta \le \delta_y) \quad (8) \\ \dfrac{\tau_y}{\delta_u - \delta_y}(\delta_u - \delta) & (\delta_y \le \delta \le \delta_u) \quad (9) \end{cases}$$

For cut-off model, the relationship is

$$\tau = \frac{4\tau_y}{\delta_u} \cdot \delta \ (0 \le \delta \le 0.5\delta_u) \tag{10}$$

The fundamental equations for the bonding and delaminating behavior of the CF sheet-concrete system are derived from Eqs. (3), (4), (5), and (7) through (10). For the rigorous procedure are

$$E_{cf} \cdot t_{cf} \cdot \frac{d^2u_{cf}(x)}{dx^2} - \frac{\tau_y}{\delta_y} u_{cf}(x) = 0 \quad (0 \le \delta \le \delta_y) \tag{11}$$

$$E_{cf} \cdot t_{cf} \cdot \frac{d^2u_{cf}(x)}{dx^2} - \frac{\tau_y}{\delta_u - \delta_y}(\delta_u - u_{cf}(x)) = 0 \quad (\delta_y \le \delta \le \delta_u) \tag{12}$$

The equation for the simplified analysis is

$$E_{cf} \cdot t_{cf} \cdot \frac{d^2u_{cf}(x)}{dx^2} - \frac{4\tau_y}{\delta_u} u_{cf}(x) = 0 \quad (0 \le \delta \le 0.5\delta_u) \tag{13}$$

The displacement and strain of the CF sheet are obtained by solving Eqs. (11), (12), and (13) with the boundary conditions summarized in Table 4.

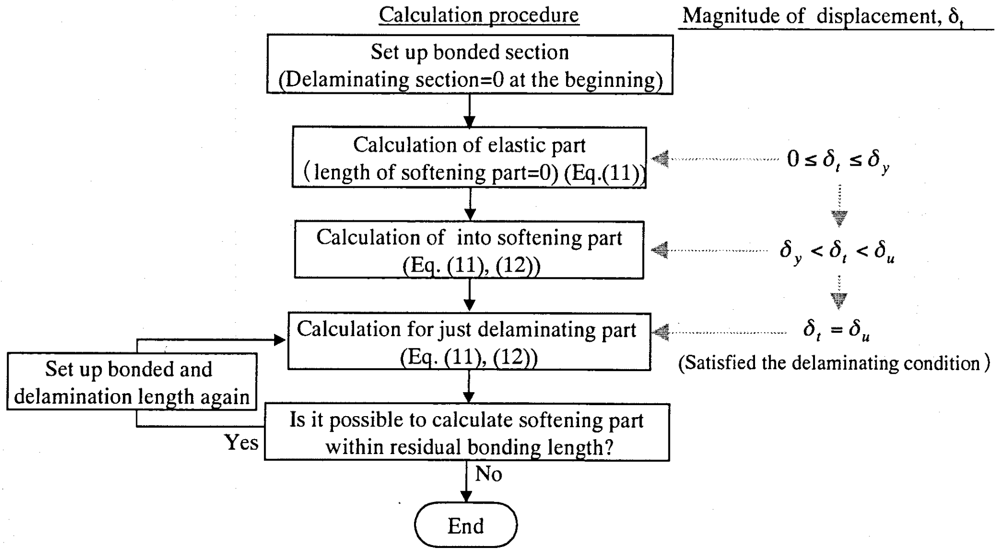

Fig. 12 Calculation flow for rigorous procedure

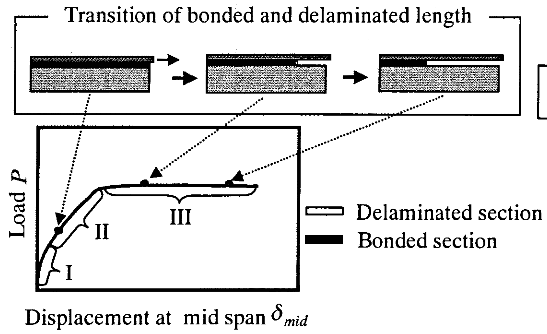

Fig. 13 Outline of simulation

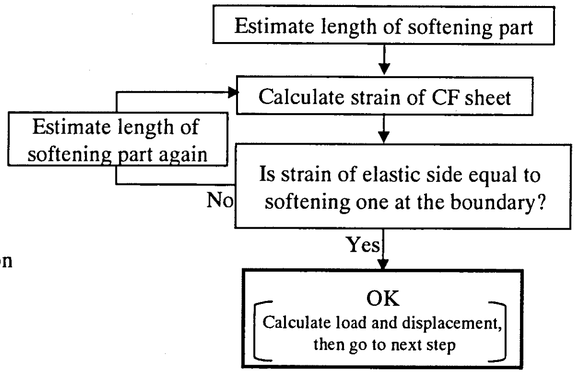

Fig. 14 Calculation flow for iteration

4.2 Bond test calculation method

a) Rigorous procedure

The computational model of the one dimensional CF sheet-concrete system is shown in Fig. 11. the model consists of a half layer as determined by the testing length of the specimen because of its symmetry. The prescribed displacement was incrementally applied to the tip of the bonded section in Fig. 12 and Fig. 13, respectively. Considering the magnitude of the prescribed displacement in correspondence with the bilinear model, the procedure was divided into three phases as follows.

Phase 1: Displacement, δ_t, is non-zero but less than δ_y. The whole bonded section corresponds to the elastic part of the bilinear model.

Phase 2: Displacement, δ_t, is greater than δ_y but less than δ_u. A softening zone is present in the tip of the bonded section.

Phase 3: Displacement, δ_t, is equal to δ_u. The delamination criterion is satisfied.

Iterative computations using the Newton-Raphson Method or similar are required to locate the correct result in Phases 2, and 3. The convergence condition is that the CF sheet strain at the tip of the elastic zone is equal to the strain at the and of the softening zone. If this condition is not satisfied, the approximated length of the softening zone is adjusted and the calculation repeated. Details of this procedure are given in Fig. 14. In the rigorous procedure, the strain and displacement of the CF sheet, the bonding stress, the applied load, and the displacement, δ_{mid}, are determined as follows.

$$P = \varepsilon_{cf}(L) \cdot E_{cf} \cdot t_{cf} \cdot b_{cf} \times 2 \tag{14}$$

$$\delta_{mid} = \frac{P}{2 \cdot E_{cf} \cdot t_{cf} \cdot b_{cf}} \times \ell_p + \delta_u \tag{15}$$

where $\varepsilon_{cf}(L)$ is the CF sheet strain at the tip of bonded section, L is the length of the bonded section, b_{cf} is the bonding width of the CF sheet, and ℓ_p is the length of the delaminated section.

To represent the propagation of delamination, the delaminated and bonded sections are updated once the delamination criterion is satisfied in Phase 3. The procedure is then repeated. Computation terminates when it is impossible to obtain the softening zone because the bonded section is too short.

b) Simplified analysis

The simplified analysis does not require iterative computation, so it is not divided into several Phases. Equation (13) is simply solved by using the procedure adopted for Phase 3.

4.3 Calculation results

a) Verification of constitutive models

The theoretical and experimental load-deflection curves at mid span for several specimens are compared in Fig. 15. The experimental curves were obtained are as follows.

Load: Data acquired from the load cell

Deflection at mid span: Obtained by integrating the strain distribution of the CF sheet from the loaded end to the specimen mid span. The integration was conducted for both faces bonded with CF sheet, and the results averaged (see Appendix).

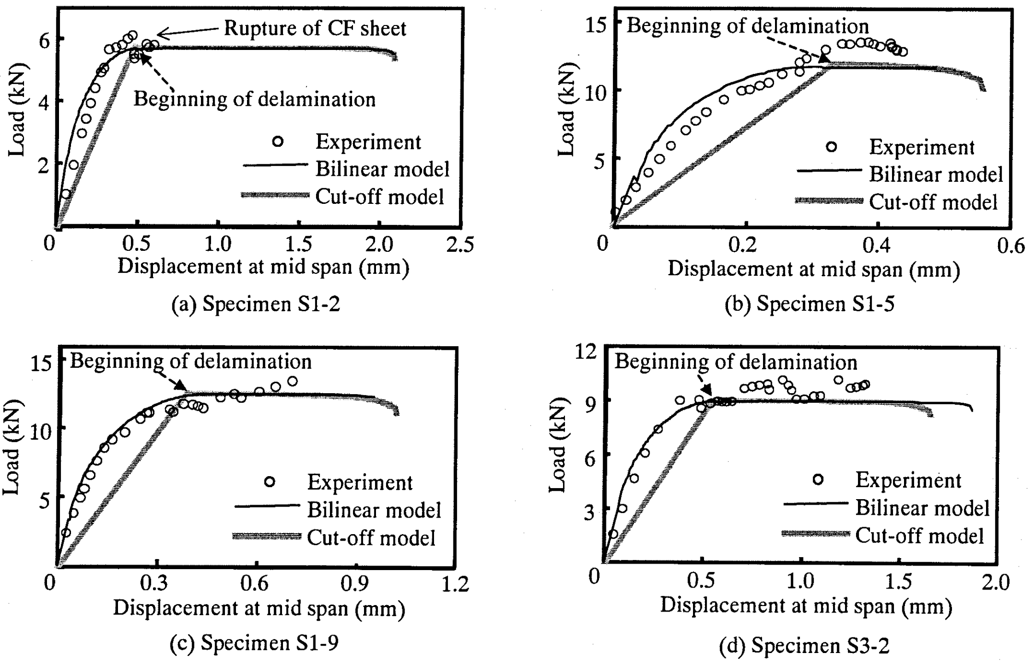

(a) Specimen S1-2 (b) Specimen S1-5 (c) Specimen S1-9 (d) Specimen S3-2

Fig. 15 Results of bond tests simulation

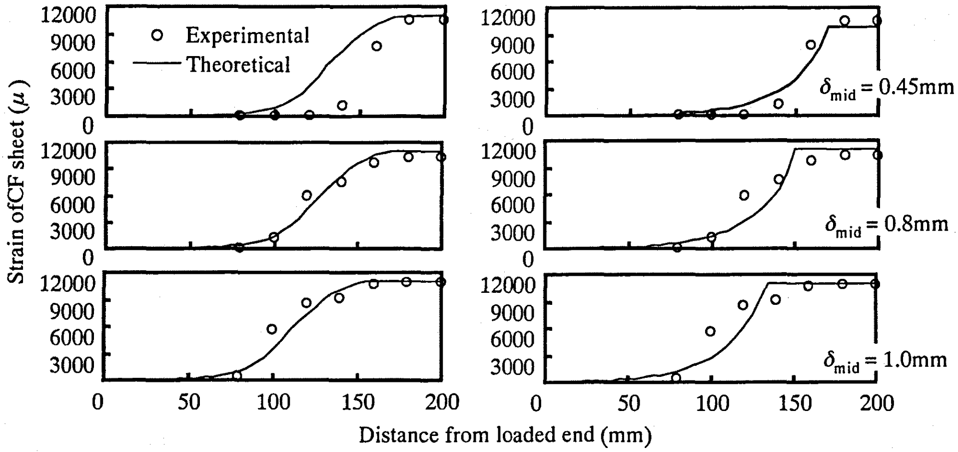

(a) Bilinear model (b) Cut-off model

Fig. 16 Comparison between experimental and theoretical strain distributions (Specimen S3-2)

Fig. 5 Material properties and boundary conditions

Concrete		Boundary conditions
Depth (mm)	Elastic modulus (kN/mm^2)	
50	28.2	$x = 0 : \sigma_{cf} = 0, x = L : \sigma_{cf} = P/t_{cf}$ for Eq. (13) $x = 0 : \sigma_c = P/t_{cf}, x = L : \sigma_c = 0$ for Eq. (16)

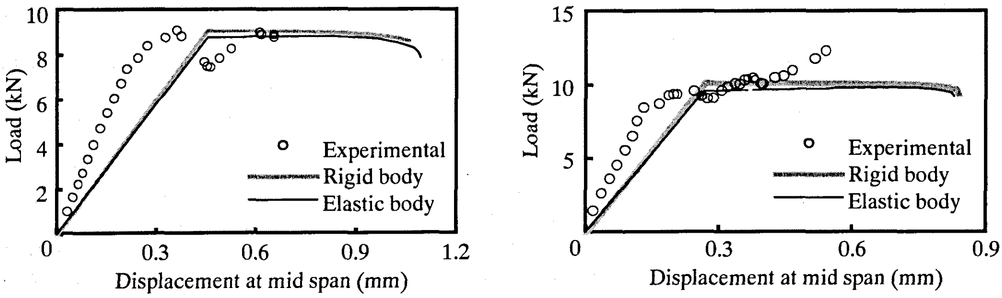

(a) Specimen S1-4 (b)Specimen S6-1

Fig. 17 Simulation results assuming that concrete is rigid and elastic body

In general, it can be seen that theoretical curves, based on the rigorous procedure, agree well with the experimental results, especially prior to delamination. Specimen S1-2 failed as a result of CF sheet rupture close to the anchored section of the specimen. Calculations, even using the rigorous procedure, are unable to predict such rupturing of the CF sheet. Further, the theoretical curves overestimate the ultimate displacement. The following experimental observation explain this: delamination propagated suddenly as the specimen failed, and the CF sheets bonded to different lateral faces of the specimen. Calculations, even using the rigorous procedure, are unable to predict such rupturing of the CF sheet. Further, the theoretical curves overestimated the ultimate displacement. The following experimental observation explains this: delamination propergated suddenly as the specimen failed, and the CF sheets bonded to different lateral faces of the specimen delaminated at different rates. The experimental curves reflect the fact that the loads may increase as a result of this behavior oncedelamination is initiated.

The theoretical and experimental curves agree well once delamination begins, even when the simplified method of analysis is used for the calculations. The theoretical and experimental strain distribution of the CF sheet are shown in Fig. 16. These distributions correspond to the magnitude of displacement at mid span. The rigorous procedure is able to accurately predict the actual strain properties, while. The simplified analysis gives very similar results.

Consequently, simplified analysis can be used to predict the actual bonding and delamination behavior of CF sheet with sufficient accuracy.
b) Corroboration of assumed concrete properties
To corroborate the assumption that concrete can be treated as a rigid body, simplified analysis was carried out for concrete as an elastic body by solving simultaneous equations (13) and (16).

$$E_c \cdot t_c \cdot \frac{d^2u_c(x)}{dx^2} + \frac{4\tau_y}{\delta_u}u_c(x) = 0 \quad (0 \le \delta \le 0.5\delta_u) \tag{16}$$

where E_c is the elastic modulus of concrete, t_c is the half depth of the specimen, and u_c is the concrete displacement. The material property of the concrete and boundary conditions for this analysis are shown in Table 5. The elastic modulus of concrete was estimated using an empirical formula[11].

The calculation results for concrete as a rigid and elastic body respectively, are shown in Fig. 17. The results obtained when it is assumed that concrete is a rigid body approximate to the elastic curve. This is expected, as concrete is a hundred times stiffer than CF sheet. (Where stiffness means the product of elastic modulus and material thickness) As a result the concrete block does not deform as much as the CF sheet when subjected to tensile force. It is clear that the assumption is appropriate in these computations.

5. CONCLUSION

In this study two derivations are proposed by which to obtain a bonding and delamination constitutive model for CF sheet bonded to concrete. The numerical calculations for simulating delaminating behavior were implemented as a sensitivity analysis on the constitutive models. The following conclusions can be drawn from this study:
(1) The shear stress and shear displacement relationships, which were derived from the strain distribution of the CF sheet obtained in the bond test, comprise elastic and softening zones.
(2) The identified parameters of the model formed the basis for the discussion of the factors influencing banding and delamination behavior. As a result, it was found that the model may be affected by the elastic modulus of the epoxy resin. The reason for this cannot be explained rationally within the scope of this study. Hopefully, future work will clarify this point.
(3) Two computational methods were used to numerically simulate the bond tests, and a rigorous procedure based on bilinear model was shown to be capable of accurately predicting the behavior of the CF sheet. A simplified analysis based on cut-off model gave similar results to the rigorous procedure.
(4) The analysis was based on the assumption that concrete is a rigid body, and this assumption was verified by carrying out simplified analysis for concrete as both a rigid and elastic body. The two sets of results were similar, indicating that concrete can be treated as a rigid body.

It is believed that proposed model is suitable for predicting the bonding and delamination behavior of CF sheet bonded on concrete.

Acknowledgements

The CF sheet was provided by Mitsubishi Chemical Co., Ltd. and Teijin Co., Ltd. The low elastic modulus epoxy resin was form Toho Earthtech Inc. The authors would like to express their gratitude to all three companies for their support.

Appendix

The crack width – namely, the displacement at mid span – was measured in the bond tests by deflection sensors. However, the integrated strain distributions from loaded end to mid span was adopted as the experimental value of displacement at mid span.

Load-displacement curves at mid span are shown in Fig. A1. This figure included a curve for an anchored specimen (Specimen S1-10) and a non-anchored specimen, respectively. Both curves are plotted with the measured displacement, and the integrated values are also are plotted. The measured and integrated displacement values do not agree in the case of the anchored specimen. The integrated value will agree with the measured displacement because concrete can be treated as a rigid body in this study (see Chapter 4). This is because the CF sheet deformation at anchored side affected to the deflection of testing length. As a result the measured displacement was greater than the actual deformation, namely, integrated value. In fact, both curves agree well in the case of non-anchored specimen.

The displacement at mid span obtained by solving Eq. (15) should be independent of deformation on the anchored side, and the integrated data is a suitable way to eliminate the effect of the anchored side in verifying the analyses.

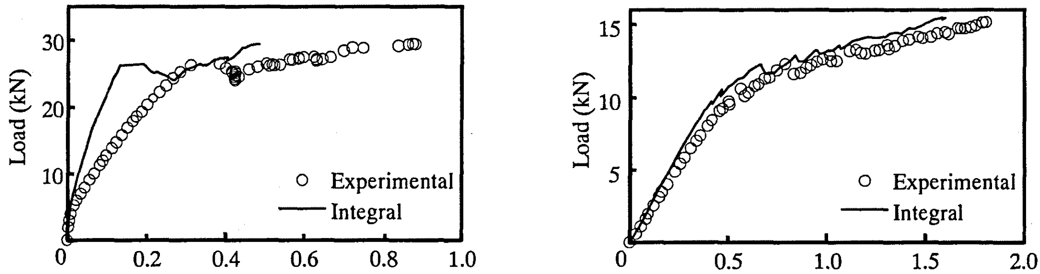

(a) Anchored Specimen (S1-10)

(b) Non-anchored specimen

Fig. 1A Comparison of anchored and non-anchored specimen displacement at mid span

References

[1] Japan Concrete Institute, "Committee Report on Continuous Fiber Reinforced Concrete", Part 1, July 1997 (in Japanese)

[2] Japan Concrete Institute, "Committee Report on Continuous Fiber Reinforced Concrete", Part 2, July 1997 (in Japanese)

[3] Japan Society of Civil Engineers Sub-Committee 307, "Design and Construction of Retrofitting Concrete Structures in Future — Tentative Draft for Performance-Based Design for Retrofitting", Concrete Engineering Series JSCE No.28, 1998 (in Japanese)

[4] Satoh, Y., Kimura, K., and Kobatake,. K., "Bond Behavior Between CFRP Sheet and Concrete (Part 1)", Journal of Structural Construction Engineering, Architectural Institute of Japan, No. 500, pp. 75-82, October 1997 (in Japanese)

[5] Wu, Z. S., Matsuzaki, T. and Tanabe, K, "Interface Crack Propagation in FRP-Strengthened Concrete Structure", *Non-Metallic (FRP) Reinforcement for Concrete Structures, Proceedings of the Third International Symposium*, Vol.1, pp.319-326, Oct. 1997.

[6] Kamiharako, A., Maruyama, K, Shimomura, T., and Nishida, H., "Evaluation of Shear Capacity of RC Beam Retrofitted with CF sheet in Consideration of Bond Characteristics", Vol. 20, No. 1, pp.497-502, July 1998 (in Japanese)

[7] Maeda,T., Asano, Y., Sato, Y., Ueda, T., and Kakuta, Y., "A Study on Bond Mechanism of Carbon Fiber Sheet", *Non-Metallic (FRP) Reinforcement for Concrete Structures, Proceedings of the Third International Symposium*, Vol.1, pp.499-506, Oct. 1997.

[8] Nishida, H., Kamiharako, A., Shimomura, T., and Maruyama, K., "Bonding Behavior of CFR sheet and Concrete", Proceedings of Japan Concrete Institute, Vol. 21, No. 3, pp.1507-1512, June 1999 (in Japanese)

[9] Kamiharako, A., Nishida, H., Shimomura, T., and Maruyama K., "A Study on Bonding Behavior of Continuous Fiber Sheet", Proceedings of 16th Annual Conference of Japan Society of Civil Engineers, Niigata Chapter, pp.11-14, November 1998 (in Japanese)

[10] Nishida H., "Bonding Characteristics on Continuous Fiber Sheet Bonded on Concrete", Masters Thesis Submitted to Nagaoka University of Technology, February 1999 (in Japanese)

[11] Japan Society of Civil Engineers, "Standard Specification for Design and Construction of Structures", March 1996